



## ISTITUTO NAZIONALE DI RICERCA METROLOGICA Repository Istituzionale

A novel magnetizer for 2D broadband characterization of steel sheets and soft magnetic composites

This is the author's accepted version of the contribution published as:

*Original*

A novel magnetizer for 2D broadband characterization of steel sheets and soft magnetic composites / O., de la Barrière; Appino, Carlo; F., Fiorillo; M., Lécrivain; C., Ragusa; P., Vallade. - In: INTERNATIONAL JOURNAL OF APPLIED ELECTROMAGNETICS AND MECHANICS. - ISSN 1383-5416. - 48:2-3(2015), pp. 239-245. [10.3233/JAE-151994]

*Availability:*

This version is available at: 11696/32656 since: 2021-02-07T07:43:58Z

*Publisher:*

IOS PRESS

*Published*

DOI:10.3233/JAE-151994

*Terms of use:*

This article is made available under terms and conditions as specified in the corresponding bibliographic description in the repository

*Publisher copyright*

(Article begins on next page)

## **A novel magnetizer for 2D broadband characterization of steel sheets and soft magnetic composites**

O. de la Barrière<sup>1a</sup>, Carlo Appino<sup>2</sup>, Fausto Fiorillo<sup>2</sup>, Michel Lécrivain<sup>1</sup>, Carlo Ragusa<sup>3</sup>, Patrice Vallade<sup>1</sup>

<sup>1</sup>SATIE, ENS Cachan, CNRS, UniverSud, 61 av du President Wilson, F-94230 Cachan, France

<sup>2</sup>Istituto Nazionale di Ricerca Metrologica (INRIM), Strada delle cacce 91, 10135 Torino, Italy

<sup>3</sup>Dipartimento di Ingegneria Elettrica, Politecnico di Torino, C.so Duca degli Abruzzi 24, 10129 Torino, Italy

---

<sup>a</sup> Corresponding author. Electronic address: [barriere@satie.ens-cachan.fr](mailto:barriere@satie.ens-cachan.fr), telephone: 0033147402125.

## Abstract

The magnetic materials used in embedded applications need characterization and modeling in the kilohertz range. This problem is well addressed under conventional alternating induction, but with rotational and two-dimensional induction loci, which are ubiquitous in electrical machines, there is lack of results, because of the difficult task of reaching such high frequencies at technically interesting induction values with the conventional laboratory test benches. To overcome this difficulty, a novel three phase magnetizer has been designed, exploiting 3D finite element calculations, and applied in the lab. This device permits one to measure magnetization curve and losses in soft magnetic steel sheets and soft magnetic composites under alternating and circular induction up to about 5 kHz. We provide a few significant examples of loss measurements in 0.20 mm thick Fe-Si and Fe<sub>50</sub>Co<sub>50</sub> laminations, and in soft magnetic composites. These measurements bring to light the role of skin effect under one- and two-dimensional fields.

## 13 I. INTRODUCTION

14 High speed electrical machines are very promising in terms of torque density [1] and are therefore interesting  
15 for embedded applications. But, in order to achieve a correct prediction of the machine efficiency at the design  
16 stage, an accurate experimental characterization of the magnetic material in the broad frequency range encountered  
17 in such machines, extending up to the kHz range, is needed.

18 Reaching high frequencies at technically significant induction levels on magnetic characterization benches is  
19 far from simple. The necessity of handling large powers with the magnetizing system is a demanding task,  
20 especially with two-dimensional (2D) fields. In such a case, no measurement standard is available, in contrast with  
21 the conventional characterization under alternating field, where one can rely, for example, on ASTM and IEC  
22 standards valid up to 10 kHz [2][3]. On the other hand, two-dimensional induction loci are ubiquitous in electrical  
23 machines [4] and the 2D magnetic characterization of soft magnetic materials has industrial relevance.

24 2D measurements are generally performed using either vertical-horizontal double-yoke magnetizers and square  
25 samples[5][6], or a three phase magnetizer with circular/hexagonal samples [7] [8]. While lack of homogeneity of  
26 the magnetic induction in the sample can be a problem [9], in all cases the test frequency at technical inductions  
27 can barely attain a few hundred Hz, far from actual frequencies encountered in high speed electrical machines.

28 We discuss in this paper design and operation of a novel 2D broadband three-phase magnetizer, by which  
29 superior performances up to the kHz range can be obtained. It is built around a laminated yoke, especially designed  
30 through 3D finite element (FEM) calculations. By this device, magnetization curve and losses in magnetic  
31 laminations and soft magnetic composite (SMC) materials under alternating and circular induction up to about 5  
32 kHz can be measured. A few significant examples of loss measurements in 0.20 mm thick Fe-Si and Fe<sub>50</sub>Co<sub>50</sub>  
33 sheets, and in SMC samples are provided and discussed.

34

## 35 II. DESIGN OF THE 2D MAGNETIZER

### 36 A) Design constraints

37 The minimum requirement formulated at start is that the three-phase magnetizer makes possible full  
38 characterization of conventional 0.20 mm thick non-oriented Fe-Si laminations under controlled 2D flux loci up

39 to peak polarization  $J_p = 1.5$  T at the frequency  $f = 1$  kHz. Instrumental to the achievement of this objective is the  
40 use of DC-20 kHz CROWN 5000VZ power amplifiers, by which each magnetizing phase can be supplied up to  
41 maximum voltage and current peak values  $V_{p,MAX} = 150$  V and  $I_{p,MAX} = 40$  A.

42

### 43 *B) Optimizing the magnetizer geometry.*

44 A schematic view of the realized three-phase magnetizer is shown in Fig. 1. For its development, the following  
45 design parameters have been imposed: 1) Circular sample of diameter  $D = 80$  mm, expected to exhibit good  
46 uniform induction profile, especially in the central region, where the induction and the effective magnetic field are  
47 measured [10]. 2) A small airgap, to minimize both the magnetizing current in each phase and the demagnetizing  
48 field. An optimal solution, taking into account the mechanical tolerances, is obtained by adopting the airgap width  
49  $a = 1$  mm. 3) Homogeneous rotating field with simplest winding configuration. To this end, the three-phase two-  
50 pole stator core was designed with three slots per pole and per phase (totalling 18 slots). To avoid winding  
51 overhang crossing, a toroidal winding configuration [11] was adopted (see Fig. 1). 4) Laminated stator core, built  
52 out of 0.35 mm thick stacked non-oriented Fe-Si sheets. The details of the windings are given in Fig. 2, where  
53 each coil occupies a slot and is series connected with all the other coils of the same phase. If  $n_s$  is the number of  
54 turns per coil (i.e. the number of conductors per slot), each phase is made of  $6 \cdot n_s$  turns in series. To achieve the  
55 desired magnetizer performances, the following geometrical parameters, shown in Fig. 1, were optimized: the slot  
56 depth  $t_s$ , the slot width  $w_s$ , the back-core thickness  $t_Y$ , and the active axial height  $T$  of the core. A convenient  
57 number  $n_s$  of copper turns per slot was assumed. With maximum magnetizing current density of  $5$  A/mm<sup>2</sup>, as  
58 required to avoid overheating, the values  $t_s = 20$  mm and  $w_s = 5$  mm are chosen. At the same time,  $t_Y$  is set to  
59 25 mm, making the maximum flux density in the back-core around 0.2 T and the associated energy losses  
60 negligible. To calculate the dependence of value and homogeneity of the generated rotating magnetic field and  
61 sample induction on the ratio between yoke height and sample thickness  $T/d$ , a 3D non-linear magnetostatic FEM  
62 modelling is implemented, where the magnetic constitutive equations of yoke sheets and test sample are identified  
63 with the corresponding experimental anhysteretic curves. When carrying out such numerical simulation, the  
64 number of turns per slot  $n_s$  is not already known, and therefore each coil is modelled by a single copper turn with

65 the magnetomotive force  $nsI_p$ . This calculated magnetomotive force per slot  $nsI_p$  providing a defined rotating peak  
66 induction  $B_p = 1.5$  T in the 0.20mm thick Fe-Si sample sheet at  $f = 1$  kHz is shown in Fig. 3 as a function of  $T/d$ .  
67 The same figure shows the corresponding trend of the peak flux, normalized to the number of turns per slot  $\Phi_p/ns$ .  
68  $\Phi_p$  is the sum of the contributions by the six series-connected coils. As expected, the required magnetomotive force  
69  $nsI_p$  decreases with increasing the ratio  $T/d$ , to reach a more or less asymptotic value beyond  $T/d \cong 80$ . Here the  
70 effect of flux fringing becomes negligible and the quantity  $\Phi_p/ns$  tends to rapidly increase with  $T/d$ , following the  
71 corresponding increase of the cross-sectional area of the core. Given these trends of  $nsI_p$  and  $\Phi_p/ns$ , their product  
72  $\Phi_p I_p$ , that is the apparent power  $\pi/\Phi_p I_p$ , passes through a minimum. This occurs for  $T/d \cong 75$  (corresponding to  $T =$   
73 15 mm), where the normalized flux  $\Phi_p/ns \cong 2$  mWb and  $nsI_p \cong 100$  A. Consequently, one obtains that the normalized  
74 peak voltage at 1 kHz is  $V_p/ns = 2\pi/\Phi_p/ns \cong 12.6$  V. With  $I_p = 10$  A and  $ns = 10$ , the voltage drop  $V_p = 127$  V is  
75 safely within the power supply capabilities. Higher frequencies can actually be reached by changing  $ns = 10$  to  $ns$   
76  $= 5$  via a mid-point connection predisposed on each coil. The accordingly built three-phase magnetizer, which is  
77 endowed with an air-cooling system, is shown in Fig. 4. It has been tested using a calibrated hysteresisgraph-  
78 wattmeter, where a defined 2D induction loci can be imposed by digital feedback [12]. Fig. 5 compares recorded  
79 and FEM calculated current and voltage waveforms in one phase of the magnetizer at  $f = 1$  kHz under imposed  
80 circular induction of amplitude  $B_p = 1.0$  T. This is detected upon a 20 mm wide central region of the 80mm diameter  
81 0.20 mm thick Fe-Si sample. It is observed that the current waveform is accurately predicted by the FEM  
82 calculations, whereas the voltage drop is slightly underestimated. This is due to the fact that the actual windings  
83 have somewhat higher overhang than the idealized windings considered in the FEM analysis (see Fig. 1), because  
84 of the mechanical rigidity of the copper wire. This implies higher inductance, that is higher voltage drop, than  
85 predicted by the numerical model, but no practical consequences on the stated objectives of the design are  
86 observed.

### 87 III. RESULTS: A FEW EXAMPLES

88 Test measurements have been performed on Fe-Si and Fe-Co sheets and on soft magnetic composites with the  
89 fieldmetric method [7]. For measurements beyond a few hundred Hz, the employed  $H$ -coil is wound with well

90 separated turns, minimizing the stray capacitances. The 3D FEM analysis shows that upon the central 20 mm  
91 measuring square region of the disk samples the homogeneity of the effective field is better than 2 %.

92 The non-oriented Fe-Si and Fe-Co 0.20 mm thick sheets have been characterized under alternating and rotating  
93 field up to  $J_p = 1.55$  T at  $f = 2$  kHz and  $J_p = 2.1$  T at  $f = 5$  kHz, respectively. An example of measured alternating  
94  $W^{(ALT)}$  and rotational  $W^{(ROT)}$  energy loss behaviour versus frequency and peak polarization  $J_p$  in the Fe-Co sheets  
95 is shown in Fig. 6a. It is noted how the maximum of the rotational loss occurs at increasing  $J_p$  values with  
96 increasing the magnetizing frequency. This occurs because of the increasing proportion of the classical loss  
97 component  $W_{class}$ , which, contrary to the other components, the domain wall related hysteresis  $W_{hyst}$  and excess  $W_{exc}$   
98 losses, monotonically increases with  $J_p$  [7]. However, loss separation is not easily treated under broadband  
99 conditions, because skin effect may arise and the standard equation of the classical energy loss, which is written  
100 as  $W_{class}(J_p, f) = k \frac{\pi^2}{6} \cdot \sigma d^2 B_p^2 f$ , where  $\sigma$  is the conductivity ( $k = 1$  for alternating sinusoidal induction,  $k = 2$   
101 for circular induction) will not apply beyond a certain upper frequency  $f_{lim}$ . It is indeed interesting to see how one  
102 can easily find  $f_{lim}$  by loss separation. It is a unique simple way to detect the surge of the skin effect. According to  
103 the statistical theory of losses and the previous equation for  $W_{class}$ , it is predicted that  $W_{diff} = W_{hyst} + W_{exc}$  is  
104 proportional to  $f^{1/2}$  [13]. Fig. 6b, showing the behaviour of  $W_{diff}$  at  $J_p = 1$  T versus  $f^{1/2}$  up to  $f = 5$  kHz, shows that  
105 such a prediction is satisfied up to  $f = f_{lim} \cong 400$  Hz. Beyond this frequency,  $W_{class}$  is overestimated by the previous  
106 equation and the calculated  $W_{diff}$  strongly deviates from the  $f^{1/2}$  behavior.

107 Further experiments have been performed on SMC samples. These materials are made of bonded and pressed  
108 iron particles, typically 10  $\mu$ m to 100  $\mu$ m wide. Because of their isotropic properties, they can handle 3D fluxes,  
109 besides being attractive for high frequency applications. Fig. 7 shows an example of energy loss versus frequency  
110 measured under alternating (sinusoidal) and circular polarization up to 4 kHz, in 80 mm diameter 3 mm thick disk  
111 samples. The non-linear increase of  $W^{(ALT)}$  and  $W^{(ROT)}$  with  $f$  can be observed also in these materials. The relatively  
112 large sample thickness, required for mechanical reasons, combines with intrinsically low permeability values to  
113 impose, for a same apparent power of the magnetizing system, pretty lower  $J_p \cdot f_{max}$  products than in sheet samples.  
114 Examples of such limits are  $J_p \cdot f_{max} = 1.25$  T·1 kHz or  $J_p \cdot f_{max} = 1.0$  T·2 kHz. They are nonetheless quite larger

115 than those obtained in the recent literature (e.g.  $J_p \cdot f_{\max} = 0.77 \text{ T} \cdot 1 \text{ kHz}$ ) [14].

#### 116 **IV. CONCLUSIONS**

117 A new magnetizer, associated with digitally controlled hysteresisgraph/wattmeter, has been developed for the  
118 broadband alternating and two-dimensional characterization of soft magnetic sheets and composites deep into the  
119 kHz range. This device, largely overcoming the upper polarization and frequency limits reported so far in the  
120 literature for similar apparatus, has been designed and optimized by 3D FEM calculations. With the high frequency  
121 range made available to the 2D measurements, the skin effect in magnetic laminations under rotating induction  
122 has been unambiguously put in evidence for the first time. The non-linear increase of the energy loss with the  
123 magnetizing frequency is also demonstrated in the soft magnetic composites.

124

- 126 [1] S. Niu, S. Ho, W. Fu, and J. Zhu, *IEEE Trans. Magn.*, **48** (2012) 1007-1010.  
127 [2] IEC Standard Publication 60404-10, Methods of measurement of magnetic properties of magnetic steel sheet  
128 and strip at medium frequencies, 1988, Geneva, IEC Central Office.  
129 [3] ASTM Publication A348/A348M, Standard test method for alternating current magnetic properties of  
130 materials using the wattmeter-ammeter-voltmeter method, 100 to 10 000 Hz and 25-cm Epstein frame, 2011,  
131 West Conshohocken, PA.  
132 [4] O. Bottauscio, M. Chiampi, A. Manzin, and M. Zucca, *IEEE Trans. Magn.*, **40** (2004) 3254-3261.  
133 [5] J.G. Zhu and V.S. Ramsden, *IEEE Trans. Magn.*, **29** (1993) 2995-2997.  
134 [6] A.J. Moses, *IEEE Trans. Magn.*, **30** (1994) 902-906.  
135 [7] C. Appino, F. Fiorillo, and C. Ragusa, *J. Appl. Phys.*, **105** (2009) 07E718.  
136 [8] A. Hasenzagl, B. Weiser, and H. Pfützner, *J. Magn. Magn. Mater.*, **160** (1996) 180-182.  
137 [9] N. Nencib, A. Kedous-Lebouc, and B. Cornut, *IEEE Trans. Magn.*, **31** (1995) 3388-3390.  
138 [10] Y. Guo, J. G. Zhu, J. Zhong, H. Lu, and J. X. Jin, *IEEE Trans. Magn.*, **44** (2008) 279-291.  
139 [11] R. Qu, M. Aydin, and T.A. Lipo, "Performance comparison of dual-rotor radial-flux and axial-flux  
140 permanent-magnet BLDC machines," in *IEEE Electric Machines and Drives Conference (IEMDC)*, 2003.  
141 [12] C. Ragusa and F. Fiorillo, *J. Magn. Magn. Mater.*, **304** (2006), e568-e570.  
142 [13] G. Bertotti, *IEEE Trans. Magn.*, **24** (1988) 621-630.  
143 [14] Y. Guo, J. Zhu, H. Lu, Z. Lin, and Y. Li, *IEEE Trans. Magn.*, **48** (2012) 3112-3115.  
144

## Figures captions

Fig. 1. 3D finite element model of the three-phase magnetizer and its main geometrical parameters.

Fig. 2. Details of the three phase magnetizer windings.

Fig. 3. Magnetomotive force per slot  $nsI_p$  and resulting peak flux per turn  $\Phi_p/ns$  as a function of core to sample thickness ratio  $T/d$  for a rotating peak induction  $B_p = 1.5$  T at  $f = 1$  kHz in a 0.20 mm thick non-oriented Fe-Si sheet sample. Minimum supply power  $\pi f \Phi_p I_p$  is required for  $T/d \cong 75$ .

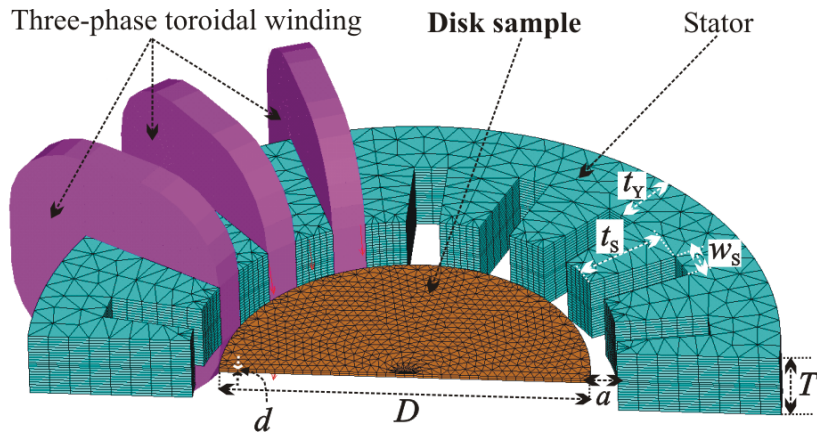
Fig. 4. The realized 2D three-phase magnetizer.

Fig. 5. Measured and FEM calculated current  $i(t)$  circulating in a phase of the stator and corresponding voltage  $v(t)$  waveforms for rotating induction  $B_p = 1$  T at 1 kHz in a 0.20 mm thick non-oriented Fe-Si sheet sample.

Fig. 6. Examples of alternating ( $W^{(ALT)}$ ) and rotational ( $W^{(ROT)}$ ) energy loss measurements performed with the novel 2D broadband magnetizer. (a)  $W^{(ALT)}$  and  $W^{(ROT)}$  measured at three different frequencies in a 0.20 mm thick Fe-Co sheet sample versus peak polarization. (b) The quantity  $W_{diff} = W - W_{class}$ , where  $W_{class}$  is the classical loss calculated according to the standard formula for uniform induction in the sample cross-section, shows strong deviation from the expected linear dependence on  $f^{1/2}$  beyond about 400 Hz, signaling the surge of the skin-effect.

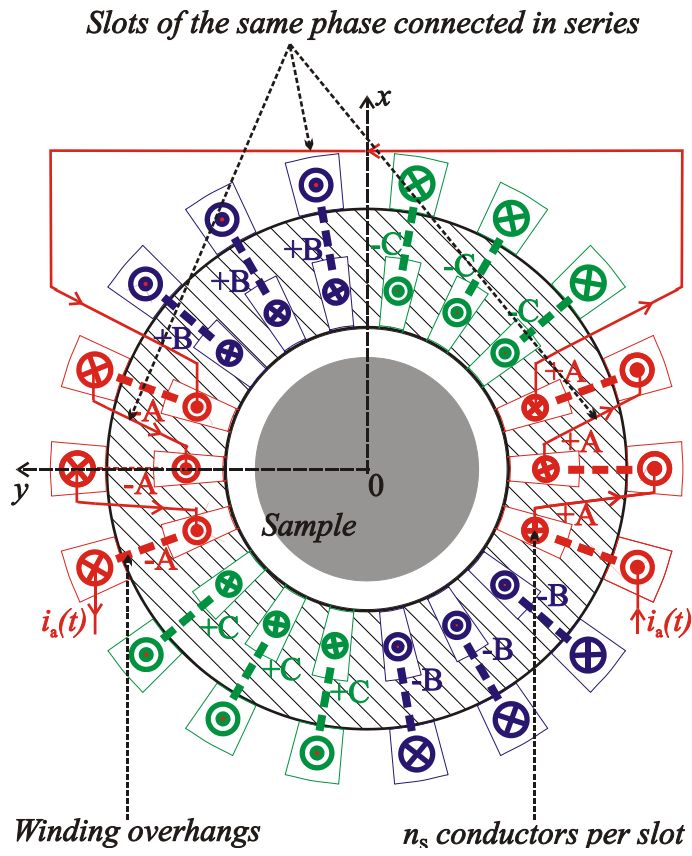
Fig. 7. Alternating and rotational energy loss versus frequency at different polarization values in a commercial soft magnetic composite. The measurements are performed on 80 mm diameter 3 mm thick disk samples.

Figures



170  
171

Fig. 1



172  
173

Fig. 2

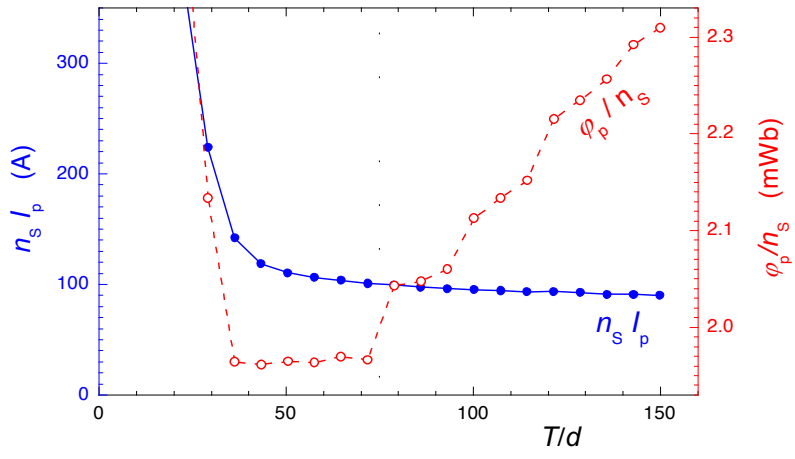


Fig. 3

174  
175

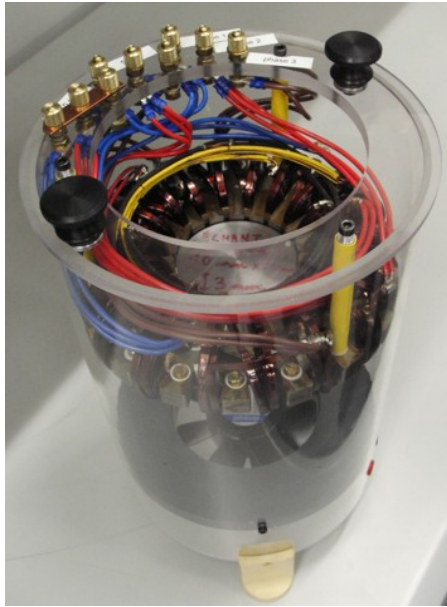
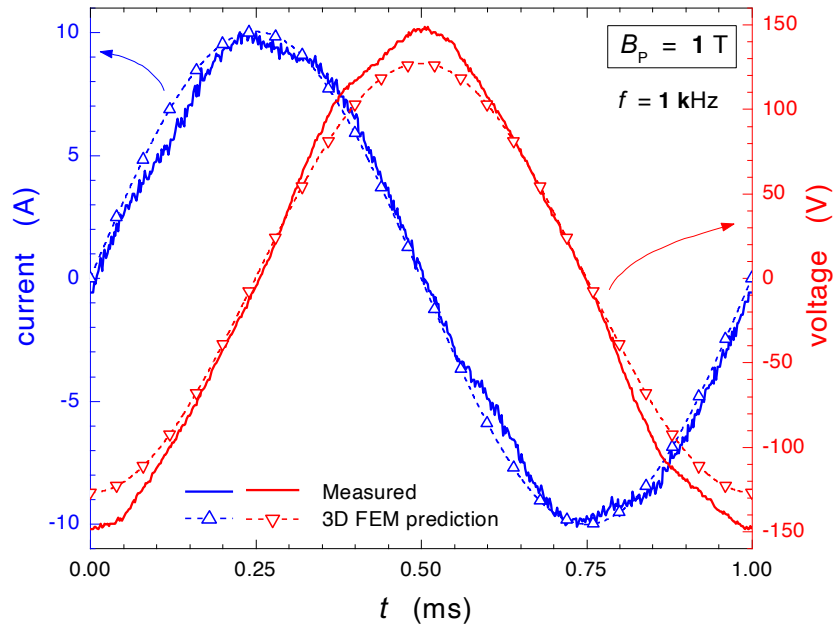


Fig. 4

176  
177



178

179

Fig. 5

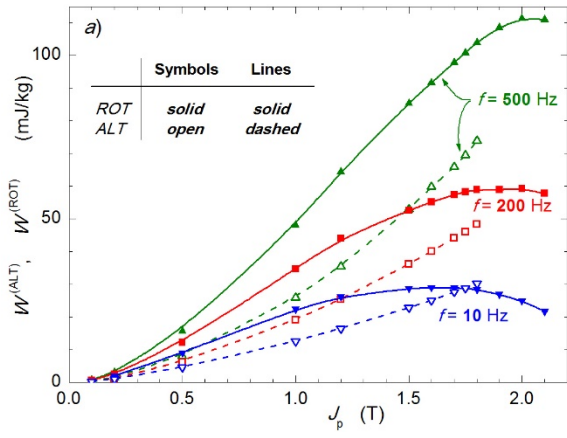
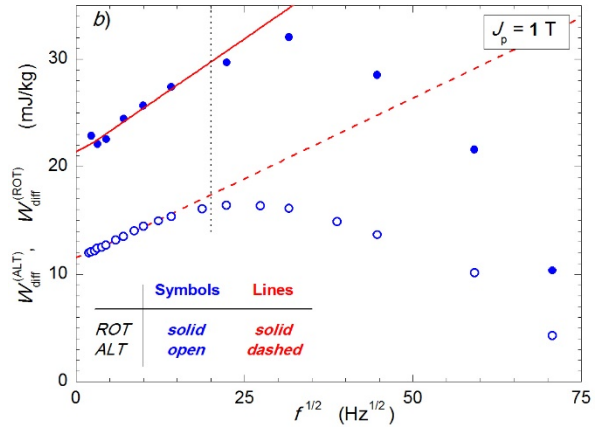


Fig. 6



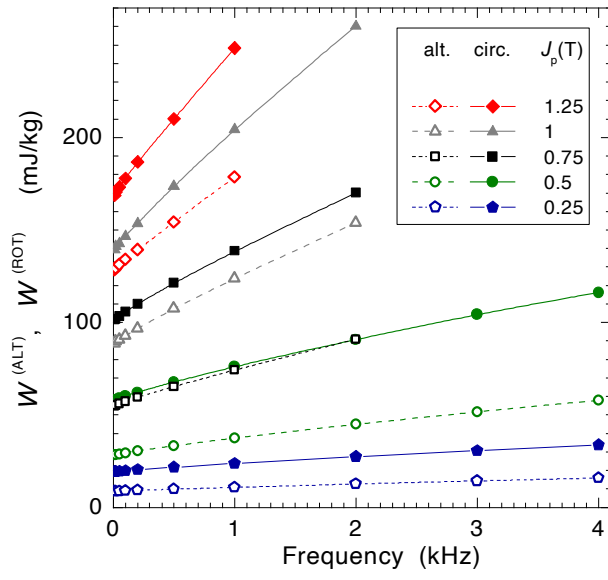


Fig. 7

181

182

183